Supplementary Information

(New Journal of Chemistry, Manuscript ID NJ-ART-10-2016-003126)

Tuning the coordination properties of multi-histidine peptides by using a tripodal scaffold: solution chemical study and catechol oxidase mimicking

Ágnes Dancs[a,c], Nóra May[b], Katalin Selmeczi[c], Zsuzsanna Darula[d], Attila Szorcsik[e], Ferenc Matyuska[a], Tibor Páli[f], Tamás Gajda[a,*]

[a] *Department of Inorganic and Analytical Chemistry, University of Szeged, Dóm tér 7, H-6720 Szeged, Hungary*

[b] *Institute of Organic Chemistry, Research Centre for Natural Sciences HAS, Magyar tudósok körútja 2, H-1117 Budapest, Hungary*

[c] *Université de Lorraine – CNRS, UMR 7565 SRSMC, BP 70239, 54506 Vandœuvre-lès-Nancy, France*

[d] *Institute of Biochemistry, Biologial Research Centre, Hungarian Academy of Sciences, Temesvári krt. 62, H-6724 Szeged, Hungary*

[e] *MTA-SZTE Bioinorganic Chemistry Research Group, Dóm tér 7, H-6720 Szeged, Hungary*

[f] *Institute of Biophysics, Biological Research Centre, Hungarian Academy of Sciences, Temesvári krt. 62, H-6724 Szeged, Hungary*

Supplementary Information content:

On the possible structure of $CuH_{-2}\mathbf{L^1}$

Since the CD spectra of $Cu\mathbf{L^1}$ and $CuH_{-1}\mathbf{L^1}$ are similar, but are very different from that of $CuH_{-2}\mathbf{L^1}$, the presence of two chiral chelate rings $\{NH_2,N_{im},N^-,NH_2\}$is probably retained after the first amide deprotonation in $CuH_{-1}\mathbf{L^1}$. The considerable differences between the UV-Vis, CD and EPR spectra of $Cu\mathbf{L^1}$/$CuH_{-1}\mathbf{L^1}$ and $CuH_{-2}\mathbf{L^1}$ (Figures 3-5) indicates the coordination of a further amide nitrogen in the equatorial plane of $CuH_{-2}\mathbf{L^1}$. This could take place in three different ways, by the formation of (*i*) $\{NH_2,N^-,N^-,NH_2\}$, (*ii*) $\{N_{im},N^-,N_{tert},N^-\}$ or (*iii*) $\{NH_2,N^-,N_{tert},N^-\}$ coordination modes in the equatorial plane of copper(II), with potential axial coordination. Option (*i*) would result in a similar binding as observed for the analogous complex of dhen [1] or 2HG [2], the only difference is the higher size of the achiral chelate ring between the two amide nitrogens. However, latter complexes, even with additional axial imidazole coordination [2], have clearly distinct UV-Vis and CD spectra as compared to that observed here, *i.e.* the large, unstable eight-membered chelate ring disfavors the formation of (*i*). In the cases of (*ii*) and (*iii*) the chiral contribution arises only from the chelate ring involving a single N-terminal His unit. Although, the differentiation between (*ii*) and (*iii*) is not self-evident, the rather unique CD spectrum determined for the species $CuH_{-2}\mathbf{L^1}$ is nearly identical to those of the $CuH_{-2}L$ complexes of Ac-HGG-NH_2, Ac-HGGG-NH_2, Ac-HGGGW-NH_2 and several other analogues of prion protein octarepeat domain [3-5]. On the other hand, the CD spectrum of the related $CuH_{-2}L$ complex of the non-protected HGG, where the coordination of the chiral chelate ring is similar to that in (*iii*) (*cf.* $\{(NH_2,N^-)*N^-,COO^-\}$ in CuH_{-2}(HGG) and $\{(NH_2,N^-)*N_{tert},N^-\}$ in (*iii*)) is considerably different from that of $CuH_{-2}\mathbf{L^1}$, it shows only a positive Cotton effect around 578 nm [3]. These facts strongly support the presence of coordination mode (*ii*) in the equatorial plane of $CuH_{-2}\mathbf{L^1}$, although the minor contribution of (*iii*) cannot be ruled out.

[1] I. Török, T. Gajda, B. Gyurcsik, G. K. Tóth and A. Péter, *J. Chem. Soc., Dalton Trans.*, 1998, 1205–1212.

[2] Ł. Szyrwiel, J. S. Pap, Ł. Szczukowski, Zs. Kerner, J. Brasun, B. Setner, Z. Szewczuk and W. Malinka, *RSC Adv.*, 2015, **5**, 56922–56931.

[3] N. I. Jakab, B. Gyurcsik, T. Körtvélyesi, I. Vosekalna, J. Jensen and E. Larsen, *J. Inorg. Biochem.*, 2007, **101**, 1376–1385.

[4] A. P. Garnett and J. H. Viles, *J. Biol. Chem.*, 2003, **278**, 6795–6802.

[5] E. Aronoff-Spencer, C. S. Burns, N. I. Avdievich, G. J. Gerfen, J. Peisach, W. E. Antholine, H. L. Ball, F. E. Cohen, S. B. Prusiner and G. L. Millhauser, *Biochemistry*, 2000, **39**, 13760–13771.

Table S1 Calculated EPR parameters of component spectra detected in the Cu(II)-$\mathbf{L^2}$ system (see also Figure 7). The component spectra (a), (b) and (c) are related to the complexes $CuH_x\mathbf{L^2}$ (x = 2, 1, 0, -1), $Cu_2H_x\mathbf{L^2}$ (x = -1, -2, -3) and $CuH_{-2}\mathbf{L^2}$, respectively.

	g_o	A_o /G	a_N	g_x	g_y	g_z	A_x /G	A_y /G	A_z /G	a_x^N	a_y^N	a_z^N
(a)	2.1121	71.5	11.6 11.6 11.6	2.0448	2.0526	2.2285	17.4	8.6	178.9	12.0 12.0 13.1	10.0 10.0 11.3	10.0 10.0 9.3
(b)	2.105	w=165 G		2.106			w=180G					
(c)	2.1117	61.8	13.9 13.9 13.9	2.097(1)	2.012(1)	2.225(1)	34.2(2)	20.0(4)	140.9(2)			

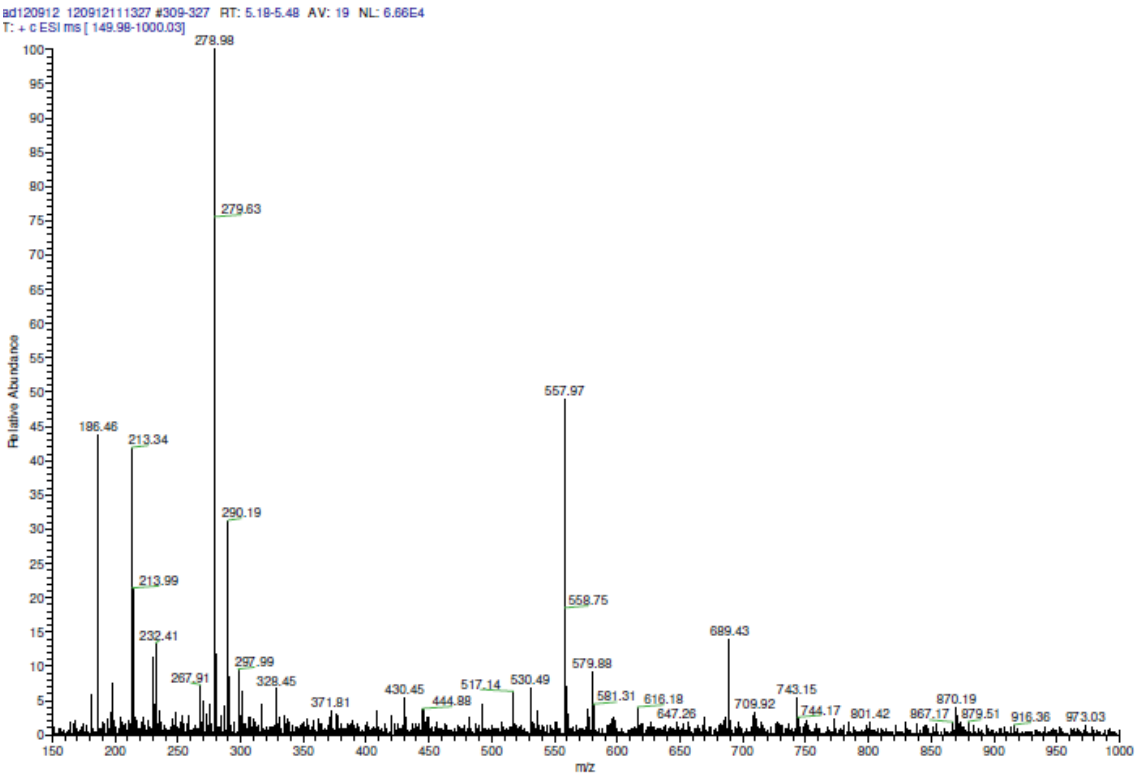

Fig. S1 ESI-MS mass spectrum of the purified ligand tren3his; *m/z* values of 557.97, 279.99 and 186.46 correspond to $[M + H]^+$, $[M + 2H]^{2+}$ and $[M + 3H]^{3+}$, respectively.

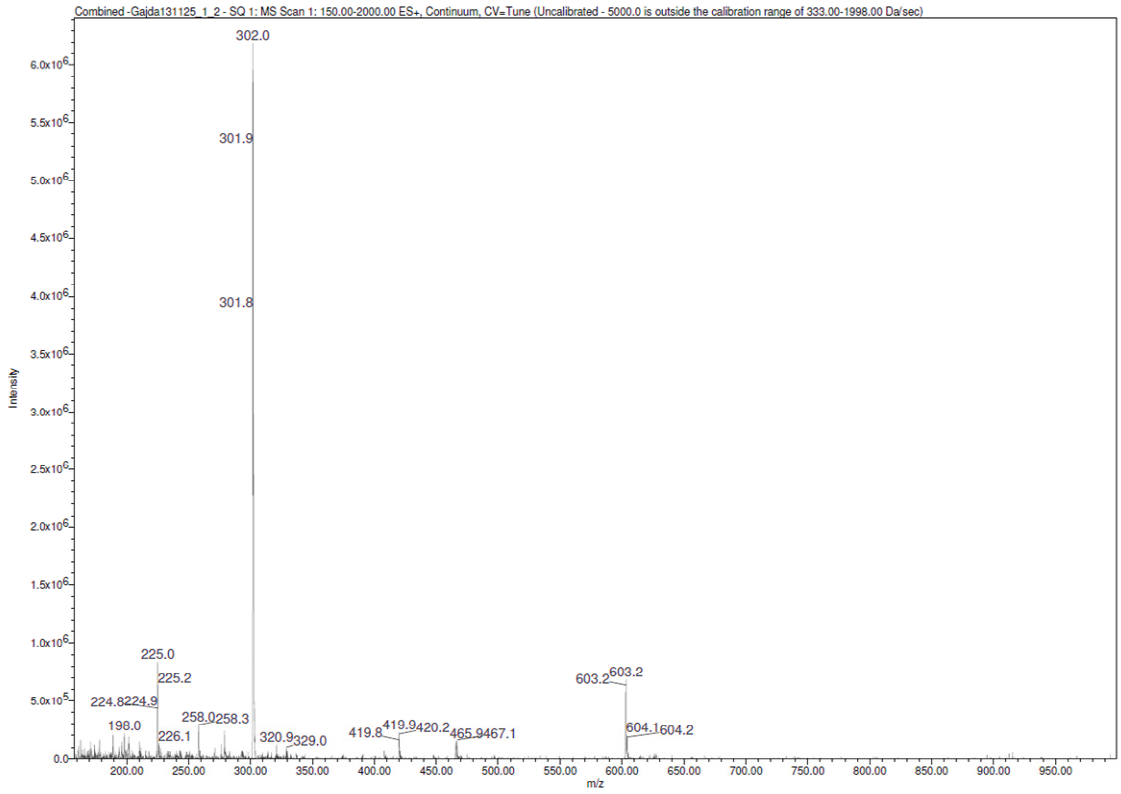

Fig. S2 ESI-MS mass spectrum of the purified ligand nta3his; *m/z* values of 603.2 and 302.0 correspond to $[M + H]^+$ and $[M + 2H]^{2+}$, respectively.

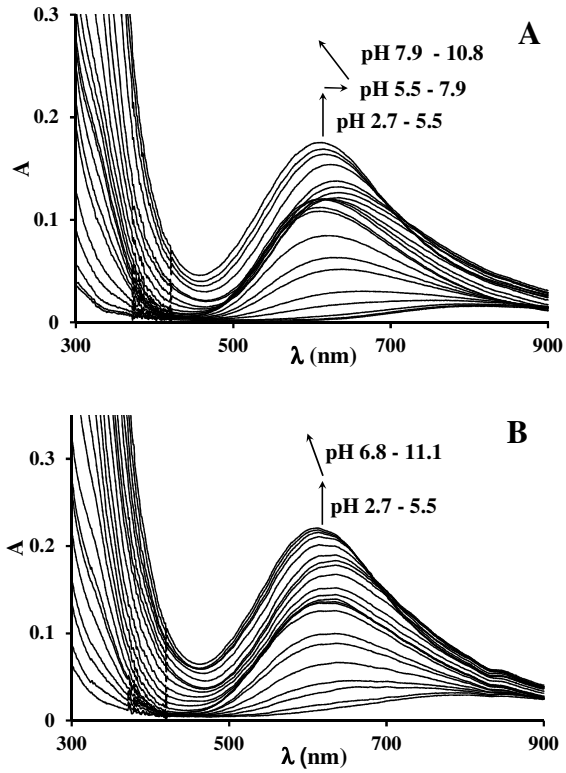

Fig. S3 pH-dependent UV-Vis spectra of Cu(II)-$\mathbf{L}^1$ 1:1 (**A**) and 3:2 (**B**) system (**A**: $c_{\mathbf{L}} = c_{Cu(II)}$ = 0.0013 M, **B**: 1.5×$c_{\mathbf{L}} = c_{Cu(II)}$ = 0.0019 M, I = 0.1 M NaCl, T = 298 K).

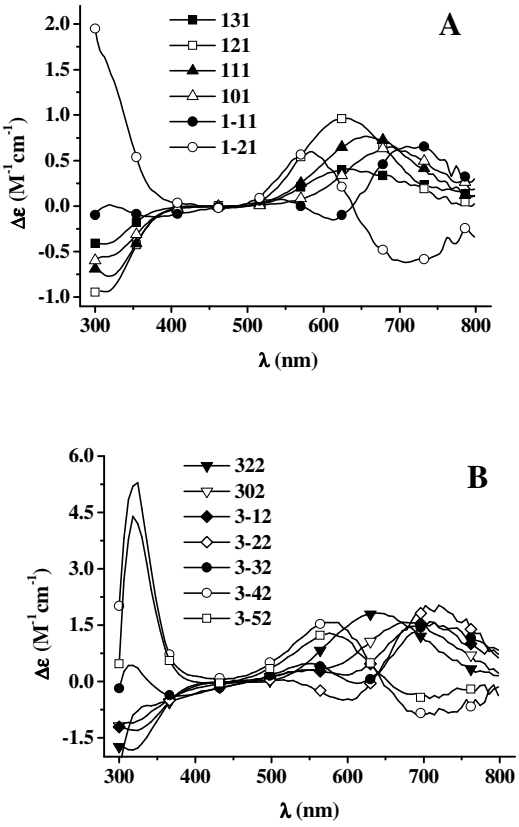

Fig. S4 Individual molar CD spectra of mononuclear (**A**) and trinuclear (**B**) Cu(II)-$\mathbf{L^1}$ complexes.

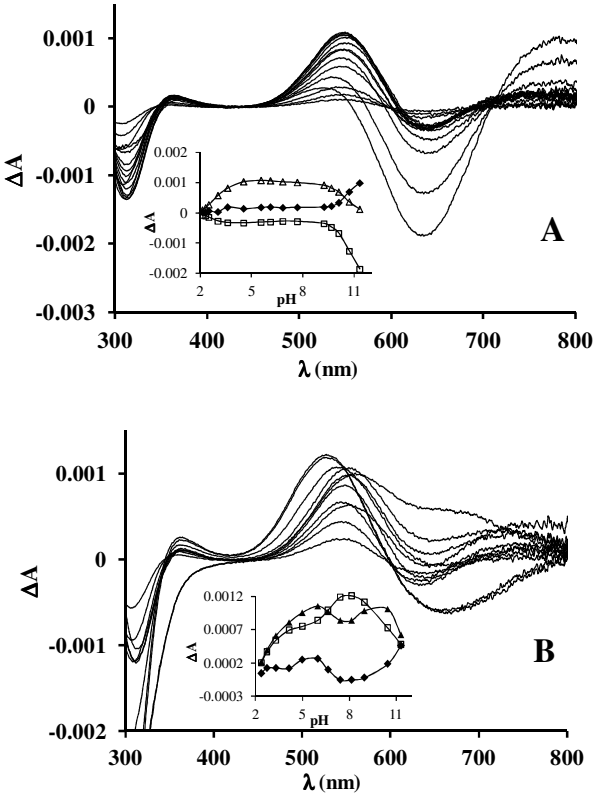

Fig. S5 Measured pH-dependent CD spectra of Cu(II)-$\mathbf{L^2}$ 1:1 (**A**) and 2:1 (**B**) system ($c_{\mathbf{L^2}}$ = 0.0016 M, $c_{Cu(II)}$ = 0.0016 M and 0.0031 M respectively, I = 0.1 M NaCl, T = 298 K). Insert: pH-dependence of Δε at: Δ 550, □ 640 and ♦ 780 nm (**A**), and □ 525, ▲ 560 and ♦ 780 nm (**B**).

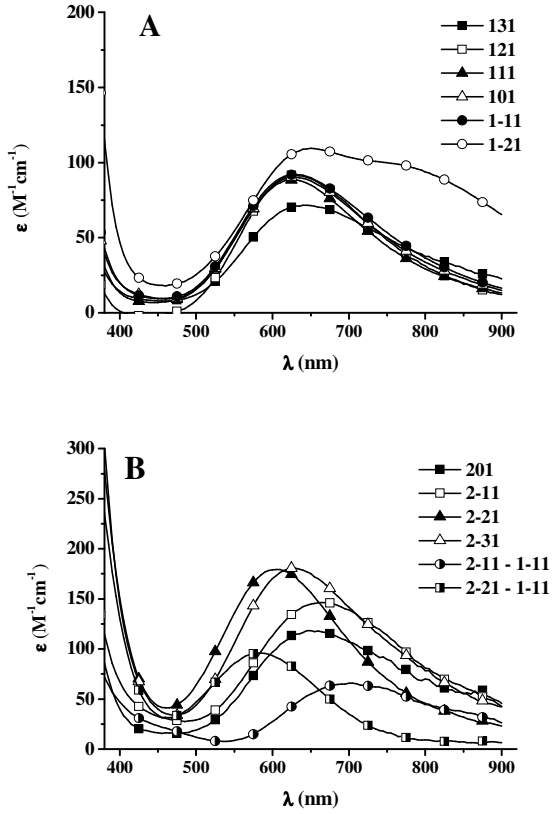

Fig. S6 Individual molar UV-Vis spectra of mononuclear (**A**) and dinuclear (**B**) Cu(II)-$\mathbf{L^2}$ complexes, along with the difference spectra of $Cu_2H_{-1}\mathbf{L^2}$-$CuH_{-1}\mathbf{L^2}$ and $Cu_2H_{-2}\mathbf{L^2}$-$CuH_{-1}\mathbf{L^2}$.

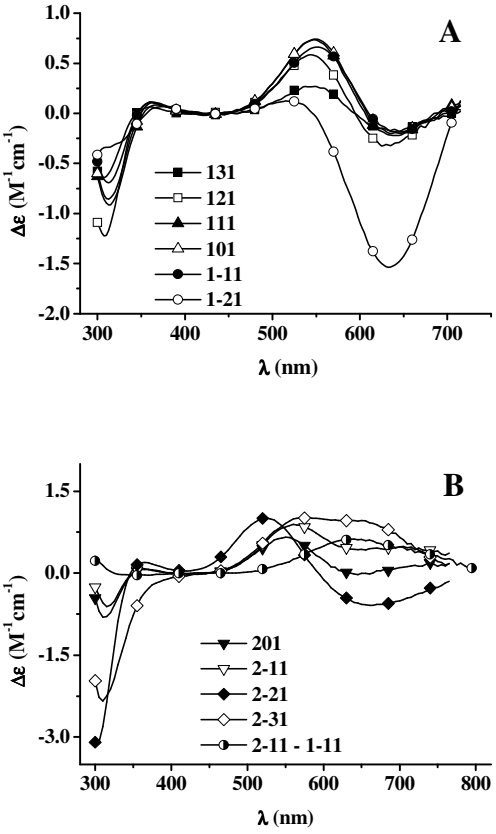

Fig. S7 Individual molar CD spectra of mononuclear (**A**) and dinuclear (**B**) Cu(II)-$\mathbf{L}^2$ complexes, along with the difference spectra of $Cu_2H_{-1}\mathbf{L}^2$-$CuH_{-1}\mathbf{L}^2$.

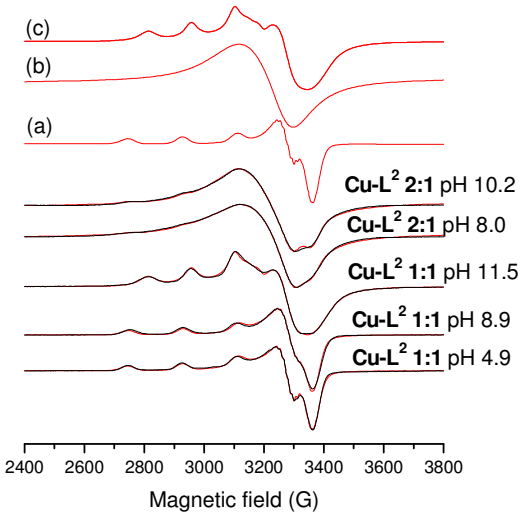

Fig. S8 Anisotropic EPR spectra recorded at 77 K in Cu(II)-$\mathbf{L^2}$ 1:1 and 2:1 systems ($c_{\mathbf{L^2}}$ = $c_{Cu(II)}$ = 0.0017 M and 1.9×$c_{\mathbf{L^2}}$ = $c_{Cu(II)}$ = 0.0033 M respectively, I = 0.1 M NaCl. Red: simulated, black: measured). Calculated EPR parameters of (a), (b) and (c) component spectra (related to the complexes $CuH_x\mathbf{L^2}$ (x = 2, 1, 0, -1), $Cu_2H_x\mathbf{L^2}$ (x = -1, -2, -3) and $CuH_{-2}\mathbf{L^2}$, respectively) are listed in Table S1.

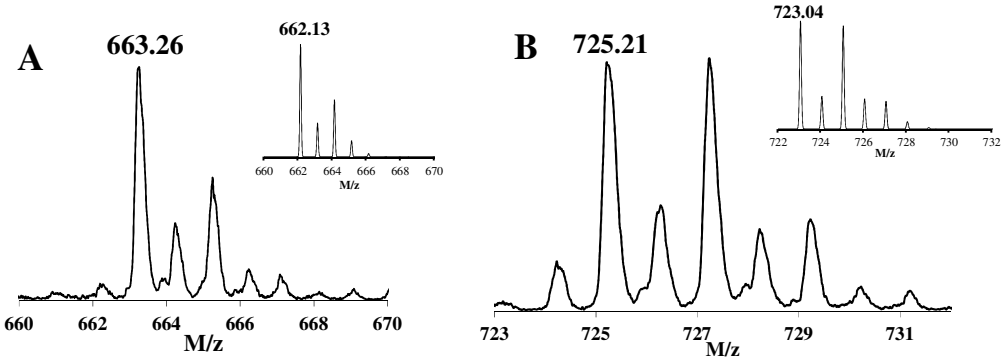

Fig. S9 MALDI-TOF MS spectra measured in the Cu(II)-$\mathbf{L^2}$ 1:1 (**A**) and 2:1 (**B**) systems. Insert: calculated spectra of the corresponding complex ($[C_{24}H_{27}N_{10}O_9Cu]^-$ and $[C_{24}H_{25}N_{10}O_9Cu_2]^-$, respectively).

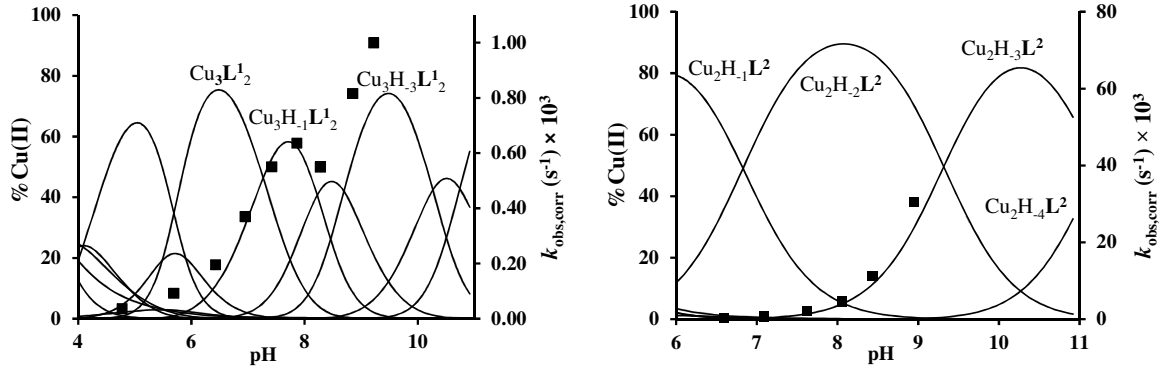

Fig. S10 pH-dependent reaction rate constants ($k_{obs,corr}$, secondary axis) at Cu(II)-$\mathbf{L^1}$ 3:2 (left) and Cu(II)-$\mathbf{L^2}$ 2:1 (right) systems with the corresponding speciation diagrams (primary axis) (c_{H_2DTBC} =1.5×10^{-3} M and 7.0×10^{-4} M, respectively, $c_{complex}$ = 5.0×10^{-5} M).

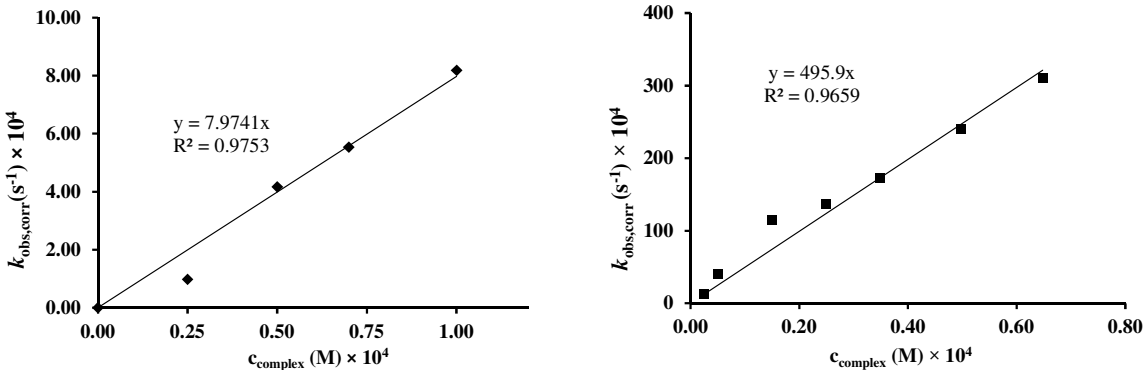

Fig. S11 Dependence of reaction rate constants ($k_{obs,corr}$) on complex concentration in Cu(II)-$\mathbf{L^1}$ 3:2 (left, pH 7.8) and the Cu(II)-$\mathbf{L^2}$ 2:1 (right, pH 8.9) systems (c_{H_2DTBC} = 5.0×10^{-3} M and 4.0×10^{-4} M, respectively).

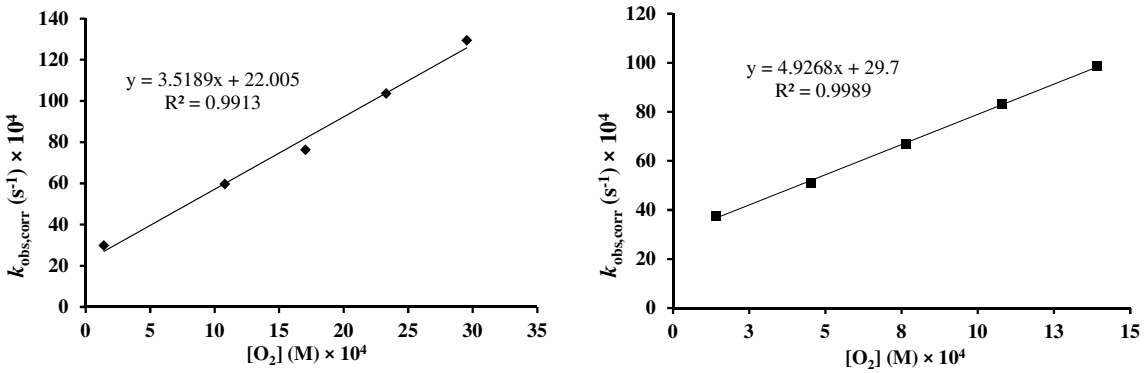

Fig. S12 Dependence of reaction rate constants ($k_{obs,corr}$) on oxygen concentration in Cu(II)-**L**^{1} 3:2 (left, pH 7.8) and the Cu(II)-**L**^{2} 2:1 (right, pH 8.9) systems ($c_{complex}$ = 4.8×10^{-5} M and 5×10^{-5} M, c_{H_2DTBC} = 5.0×10^{-4} M and 8.0×10^{-4} M, respectively).

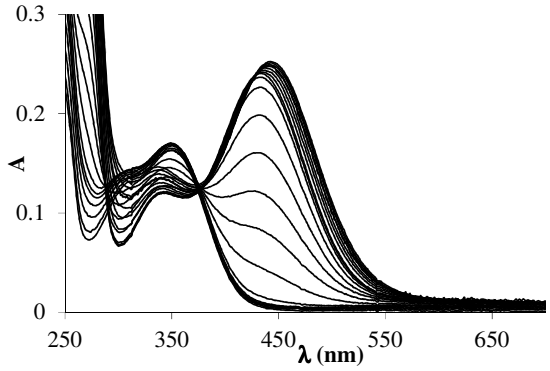

Fig. S13 UV-Vis spectra between pH 2-12 in presence of Cu(II)-**L**^{1}-H$_2$4NC 3:2:1 (c_{H_24NC} = 2.5×10^{-4} M, in EtOH/H$_2$O 50/50).

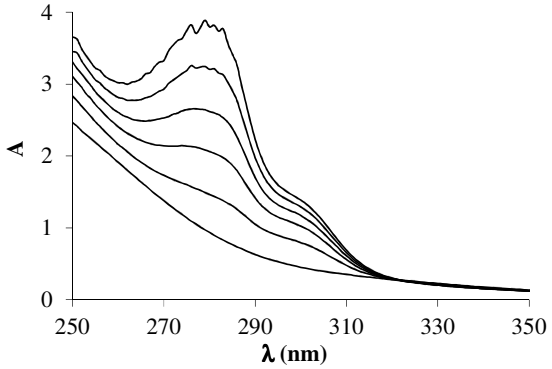

Fig. S14 UV region of H$_2$DTBC-dependent UV-Vis spectra of Cu(II)-**L**^{1} 3:2 system under anaerobic conditions ($c_{complex}$ = 2.4×10^{-4} M, in EtOH/H$_2$O 50/50, pH 7.8), in presence of 0 to 5 eq. H$_2$DTBC.

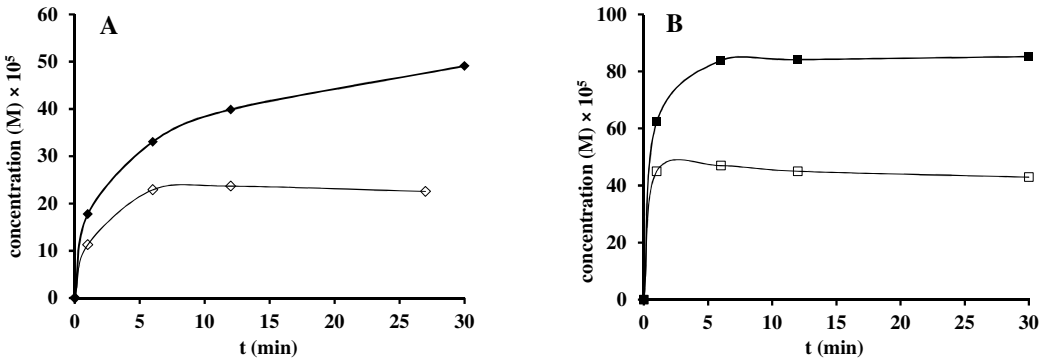

Fig. S15 H_2O_2 and DTBQ formation in presence of Cu(II)-$\mathbf{L^1}$ 3:2 (**A**) and Cu(II)-$\mathbf{L^2}$ 2:1 systems (**B**). ◊ and □: [H_2O_2] produced by the complex-catalyzed reaction (pH 7.8 and 8.5), ◆ and ■: [DTBQ] produced by the complex-catalyzed reaction (pH 7.8 and 8.5). $c_{complex} = 5\times10^{-5}$ M, $c_{H_2DTBC} = 2\times10^{-3}$ M, $I = 0.1$ M.